Neuroscience Letters 606 (2015) 36–41

Contents lists available at ScienceDirect

Neuroscience Letters

journal homepage: www.elsevier.com/locate/neulet

Research paper

# Mapping the functional connectivity of the substantia nigra, red nucleus and dentate nucleus: A network analysis hypothesis associated with the extrapyramidal system

Hong-Ying Zhang[a], Hui Tang[b], Wen-Xin Chen[a], Gong-Jun Ji[c], Jing Ye[a], Ning Wang[a], Jing-Tao Wu[a,*], Bing Guan[d,*]

[a] Department of Radiology, Subei People's Hospital of Jiangsu Province, Yangzhou University, Yangzhou 225001, China
[b] Medical Experimental Center, Subei People's Hospital of Jiangsu Province, Yangzhou University, Yangzhou 225001, China
[c] Hangzhou Normal University, Center for Cognition and Brain Disorders, Hangzhou 310015, China
[d] Department of Head and Neck Surgery, Subei People's Hospital of Jiangsu Province, Yangzhou University, Yangzhou 225001, China

## HIGHLIGHTS

- We firstly described the architectures of the extrapyramidal networks with resting-state functional analysis.
- The extrapyramidal related regions constituted a relatively exclusive network.
- Study on the extrapyramidal system networks has potential clinical implications.

## ARTICLE INFO

*Article history:*
Received 19 April 2015
Received in revised form 13 August 2015
Accepted 17 August 2015
Available online 2 September 2015

*Keywords:*
Functional MRI
Extrapyramidal system
Low frequency fluctuations
Brain networks

## ABSTRACT

This study aimed to examine the functional networks related to the extrapyramidal system using a temporal oscillation signal correlation analysis method based on critical nodes in the substantia nigra (SN), red nucleus (RN) and dentate nucleus (DN). Nineteen healthy subjects underwent resting-state fMRI and susceptibility weighted imaging (SWI). For the brain network analysis, the SN, RN and DN were positioned on susceptibility weighted images and used as seeds for temporal correlations analyzed via BOLD data. *T*-tests were performed for the correlation coefficients of each seed. We demonstrated that the SN, RN and DN were functionally connected to each other, and, in general, their connectivity maps overlapped in a series of subcortical extrapyramidal structures and regions of cerebral cortices. A Granger causality analysis indicated that the effective connectivity graphs within extrapyramidal structures mainly exhibited a spacial up-down pattern for the positive and negative influences, respectively. Our findings suggest that extensive regions involved in the extrapyramidal system constituted a relatively exclusive network via spatial-temporal correlation signals that analogously corresponded to the anatomical structures. The investigation of extrapyramidal system networks may have potential clinical implications.



## 1. Introduction

The extrapyramidal system is critical for the control and modulation of motor function and gesture retention. Traditionally, the extrapyramidal system has comprised a set of brain regions, including the cerebellum, dentate nucleus (DN), substantia nigra (SN), red nucleus (RN), thalamus, striatum and regions of the cerebral cortex [1,2]. These regions collaborate with each other to perform targeted functions. The extrapyramidal system comprises complicated and dense anatomical circuits; however, the functional correlations among the extrapyramidal components remain unclear.

The measurement of low frequency fluctuations (LFFs) in blood oxygen level-dependent (BOLD) functional magnetic resonance imaging (fMRI) signals has been widely used to map intrinsic brain networks. Functional connectivity implies cooperative correlations of low frequency fluctuations (LFFs) in fMRI signals among spatially distant brain regions. Using resting state fMRI, multiple brain networks have been associated with high-order cognitive functions, including the default mode, dorsal attention, executive control

* Corresponding authors. Fax: +86 514 87937563.
*E-mail addresses:* wujingtaodoctor@126.com (J.-T. Wu), aliceguan0685@sina.com (B. Guan).

http://dx.doi.org/10.1016/j.neulet.2015.08.029
0304-3940/

and salience networks [3–5], as well as sensory and motor function related networks [6,7]. In a broad spectrum of populations, resting-state fMRI studies have demonstrated moderate-to-high test-retest reliability and reproducibility for large-scale brain networks using different methods for data processing, including seed-based, independent component analyses (ICA) and graph theoretical approaches [8,9]. A high functional connectivity within resting-state networks supports the influence of direct or indirect anatomical connections [10–12].

fMRI studies have investigated the functional connectivity of specific subcortical structures, such as the thalamus [13], basal ganglia [14,15], periaqueductal gray [16], red nucleus and substantia nigra [17]. These findings have substantially enhanced our understanding of the intrinsic networks of subcortical brain structures. The subcortical brain networks in previous studies have been examined with ICA or seed-based temporal correlation methods; however, these networks only embraced parts of subcortical and cortical structures and cannot mimic the extrapyramidal network. To date, no other resting-state fMRI analysis methods have been applied to investigate subcortical networks likely because of the methodological limitations.

A novel technique referred to as magnetic resonance susceptibility weighted imaging (SWI), which identifies the magnetic susceptibility differences of tissues, could provide a good approach to visualize the subcortical nuclei. Using SWI, the DN, SN and RN structures exhibit sharp delineations because of physiological iron deposition [18]. SWI images co-registered with fMRI images enable the exact extraction and calculation of fMRI signals in these nuclei.

The SN, RN and DN are important intermediate nodes in the extrapyramidal system, and these regions exhibit complicated afferent and efferent anatomical fiber tracts connected to other extrapyramidal regions. As a result of the dense and complicated anatomical circuits and projections within the extrapyramidal system, we hypothesized that all extrapyramidal regions should converge into a strong, functionally intraconnected network.

To date, few studies have focused on the SN, RN and DN networks; for example, Nioche et al. demonstrated that the resting-state brain networks were related to the SN and RN using a seed-based temporal correlation analysis method, in which the seeds were directly manually defined on the original BOLD images [17]. Wu et al. compared the Granger causality effects from the SN to the basal ganglia and cortex between PD patients and controls [19]. One drawback of these previous approaches is that the regions of interests (ROIs) were positioned directly on the BOLD images, which resulted in poorly defined ROIs because the original BOLD images had low resolutions and indistinct signal features. In the current study, we improved this method via ROI extraction from SWI, which provided excellent ROI identification. We expect the improved method to better extract the associated brain networks.

The aim of the current study was to investigate the network associated with the extrapyramidal system via the analysis of resting-state LFFs based on the bilateral seed regions of the RN, SN and DN. If the extrapyramidal regions linked into a network by the cooperative LFFs, our second aim was to further understand the connectional directionality among the extrapyramidal structures.

## 2. Materials and methods

### 2.1. Subjects and data acquisition

Nineteen healthy right-handed subjects were recruited from local university students (aged 22–33 years, mean 24.9 ± 1.8 years; 10 males, 9 females). All subjects underwent a structural brain MRI and had no abnormal findings. This study was approved by the university ethics committee. All subjects provided written informed consent prior to scanning.

The subjects wore headphones and were instructed to lie in a supine position in a standard head coil of a 3.0T GE Signa HDx MR scanner (GE Healthcare systems, Milwaukee, WI, USA). Prior to the resting-state fMRI, the subjects were instructed to relax with their eyes closed and to not to think of anything in particular. Functional images were acquired using a gradient echo-planar imaging (EPI) sequence with the following parameters: TR 2000 ms, TE 30 ms, flip angle 90, slice thickness 4 mm, slice gap 0 mm, FOV 240 mm and matrix 128 × 128; each frame included 35 continuous slices that covered the whole brain volume. The slices were parallel to the anterior/posterior commissure. The EPI scan lasted 5 min. To provide an anatomical reference, a T1 weighted three dimensional (3D) high resolution IR gradient-echo sequence that covered the whole brain was acquired with the following parameters: TR 12 ms, TE 5.1 ms, TI 450 ms, flip angle 20, slice thickness 1 mm, slice gap 0 mm, FOV 256 mm and matrix 256 × 256. Finally, 3D high resolution SWI was performed with the following sequence parameters: TR 68 ms, TE 6.5 ms, slice thickness 2 mm, FOV 240 mm and matrix 416 × 356; the 3D slab thickness was 120 mm, which covered most of the cerebellum and cerebrum.

### 2.2. Data preprocessing and analysis

fMRI data preprocessing was performed with DPARSFA v 2.3 software (http://www.restfmri.net) implemented in MATLAB. The first four volumes were discarded. The images were corrected for slice-timing and subsequently realigned for rigid-body head movement correction. To minimize movement artifacts, individuals with translations that exceeded 1.5 mm in any direction or head rotation that exceeded 1.5° in any angle were excluded ($n = 3$). The functional images were subsequently normalized using DARTEL. T1 weighted 3D images were segmented into three modulated, normalized components of grey mater, white matter and cerebrospinal fluid (CSF). Considering the close spatial distance between the RN and SN and the tiny subcortical nucleus volume, we re-sampled the normalized volumes into a voxel size of 2 mm × 2mm × 2 mm in Montreal Neurological Institute (MNI) space. The EPI images were spatially smoothed using an isotropic Gaussian filter (4 mm FWHM). The head movement parameters (Friston 24-parameter model [20] and the white mater, CSF, and global mean signals were regressed out. Recent studies have suggested that the signal spike caused by head motion significantly contaminated the final fMRI connectivity results even after regressing out the linear motion parameters [21]. Thus, the fMRI data further regressed out spike volumes when the frame-wise displacement of the specific volume exceeded 0.5. Linear detrending and temporal bandpass filtering (0.01–0.08 Hz) were conducted.

The SWI magnitude images were co-registered to the 3D T1 image and normalized to the MNI space using SPM5 (http://www.fil.ion.ucl.ac.uk/spm); we selected seed regions by drawing the ROI on an individual SWI. Bilateral RN, SN and DN regions appear as strong hypointense signals on the SWI magnitude images and are easily identifiable (Fig. 1); the gaps between the RN and SN are sufficiently wide to avoid overlap. The ROIs of the bilateral RN, SN and DN comprised the seed regions for each subject using MRIcron software.

### 2.3. Functional connectivity analysis

A functional connectivity analysis was performed using the Resting-state fMRI data Analysis Toolkit (REST V1.8, http://www.restfmri.net/forum/rest). Positive linear correlation coefficients between each brain voxel and the mean time series of each seed region were calculated. A Fisher's $z$-transformation was applied

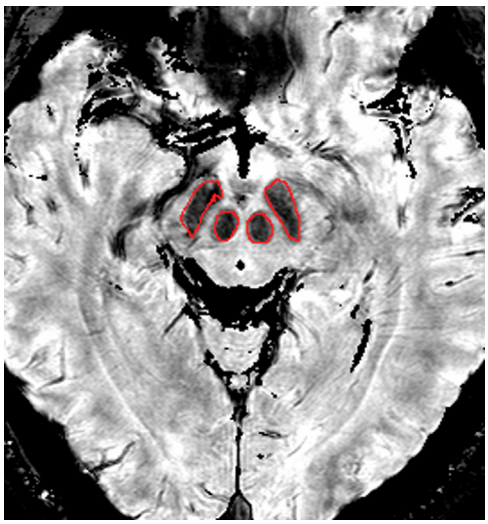

**Fig. 1.** Illustration of the seed positions for the substantia nigra and red nucleus. The seed regions are clear in susceptibility weighted imaging (SWI) and are manually drawn (outlined) on the individual image. (For interpretation of the references to color in this figure legend, the reader is referred to the web version of this article.)

to improve the normality of these correlation coefficients. The individual $z$ maps were entered into two-tailed, random-effects, one sample $t$-tests to identify the brain areas that exhibited functional connectivity across subjects. The threshold corrected with AlphaSim was set at $p < 0.001$ with a voxel wise $p < 1 \times 10^{-6}$, a cluster size >34 voxels (272 $mm^3$) and a cluster connectivity criterion of 5 rmm.

### 2.4. Effective connectivity analysis

We evaluated the effective connectivity between the extrapyramidal regions via Granger causality analysis (GCA). The nodes involved in the RN, SN and DN networks were selected and entered into REST V1.8 toolkit to analyze granger causality effects. The node coordinates were based on local activation peaks with a 6 mm radius on the prior one sample $t$-test. The RN, SN and DN ROIs were directly used as the nodes because of their small size. Bivariated signed path coefficient maps comprised the output. Effective connectivity graphs were constructed using the connecting lines labeled with weights and arrows to indicate the strengths and directions of the causal influences, respectively.

## 3. Results

As shown in Figs. 2–4, the RN, SN and DN demonstrated functional coherence with each other, and their connectivity maps largely overlapped in regions that included the pars dorsalis pontis, subthalamic nucleus, insular lobe, dorsal thalamus, putamen, globus pallidus, head of the caudate nucleus, supramarginal gyrus and dorsal anterior cingulate cortex (dACC). In addition, the SN network exhibited connectivity with the supplementary motor area (SMA). The DN network exhibited connectivity with the vermis, and both the RN and SN exhibited significant connectivity with the precuneus. For the bilateral seeds of the RN, SN and DN, the connectivity maps globally presented symmetric and similar patterns.

GCA was performed to determine the ROI-wise signed-path coefficients among the 16 involved brain network nodes. Positive and negative signed-path coefficients indicate that previous brain region values predict increased and decreased activity, respectively, of the present value of another region [22,23]. Sixteen cortical and subcortical ROIs were selected: paired ROIs of the SN, RN and DN that originated from above the manual course, bilateral ROIs of the thalamus, putamen, globus pallidus, dACC and SMA derived from the one-sample $t$ test, which were defined as spheres with a 6 mm radius centered at the coordinates of the peak T voxels. Bivariated signed-path coefficients were calculated between any two ROIs. The coefficients were analyzed via a one sample t-test with a threshold set at corrected $p < 0.05$. Only the links that exhibited significant effective connectivity were presented on the

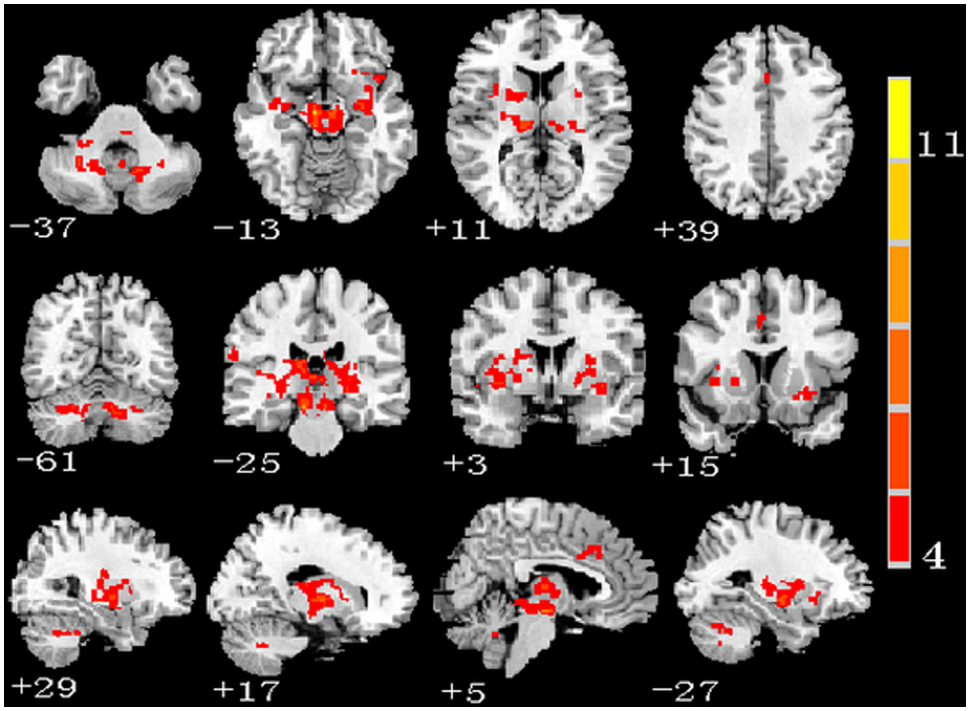


**Fig. 2.** Intra-group connectivity map of the red nucleus. The color bar denotes $T$ values. The statistical threshold was set at $p < 0.001$, corrected with AlphaSim. (For interpretation of the references to color in this figure legend, the reader is referred to the web version of this article.)

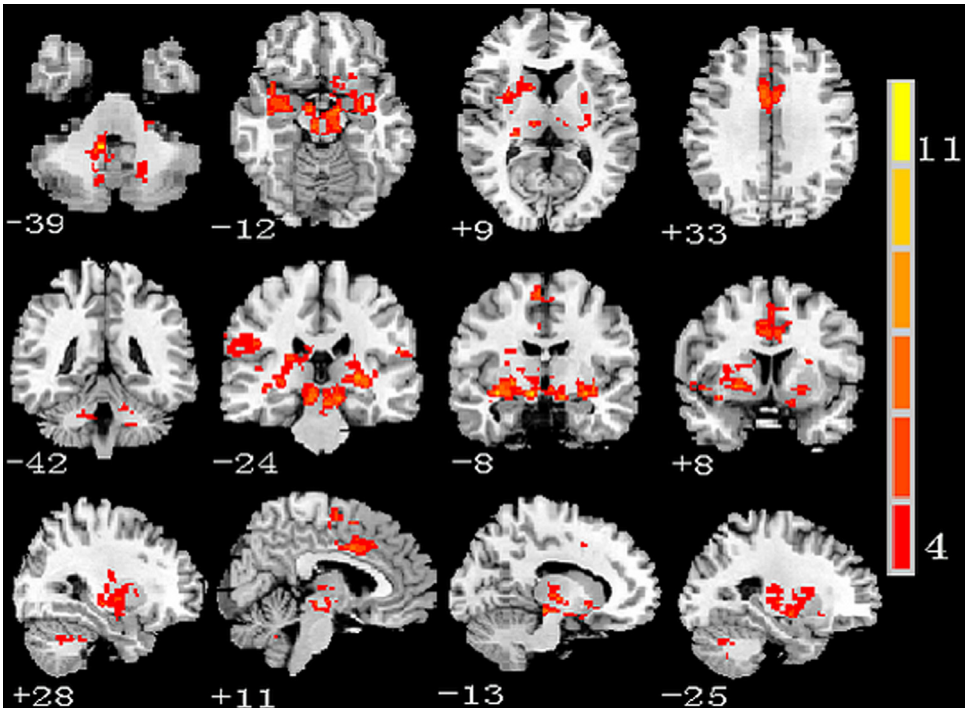


**Fig. 3.** Intra-group connectivity map of the substantia nigra. The color bar denotes *T* values. The statistical threshold was set at $p < 0.001$, corrected with AlphaSim. (For interpretation of the references to color in this figure legend, the reader is referred to the web version of this article.)

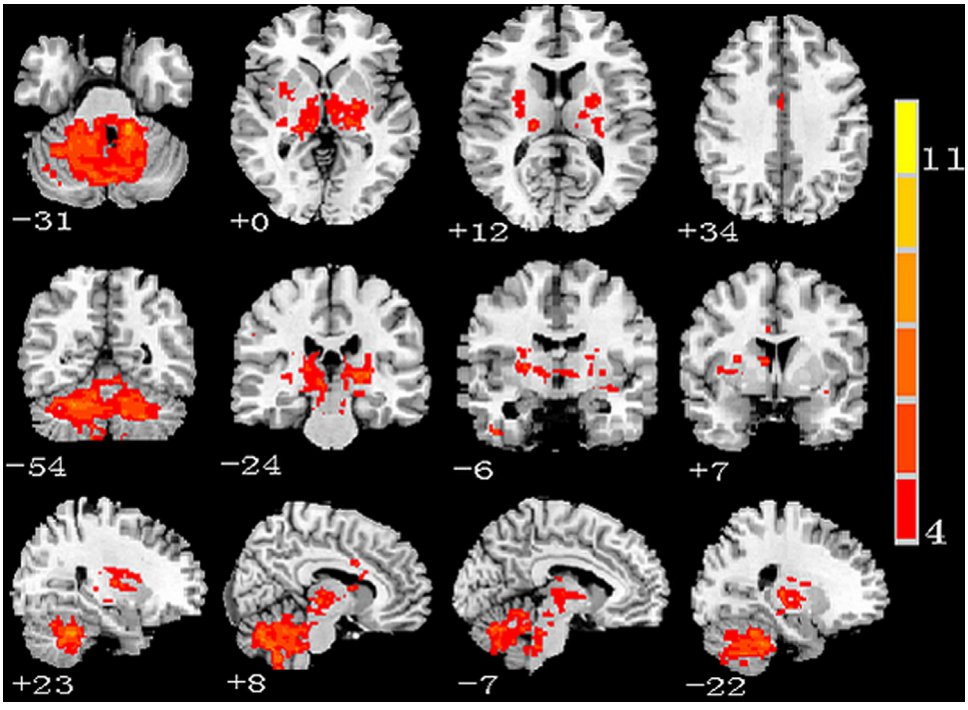


**Fig. 4.** Intra-group connectivity map of the dentate nucleus. The color bar denotes *T* values. The statistical threshold was set at $p < 0.001$, corrected with AlphaSim. (For interpretation of the references to color in this figure legend, the reader is referred to the web version of this article.)

network map (Fig. 5). In general, the Granger causal connectivity maps presented an up-down pattern for positive and negative influences, respectively; thus, a negative influence primarily presents from the superior to inferior space, whereas a positive influence primarily exhibits the opposite pattern. Subcortical nuclei predominately exhibited positive influences on motor cortices, such as the bilateral putamen to the SMA and dACC, the left SN to the left dACC and the left DN to the right dACC.

## 4. Discussion

Although the functional connectivities of subcortical regions have previously been systematically examined, investigations

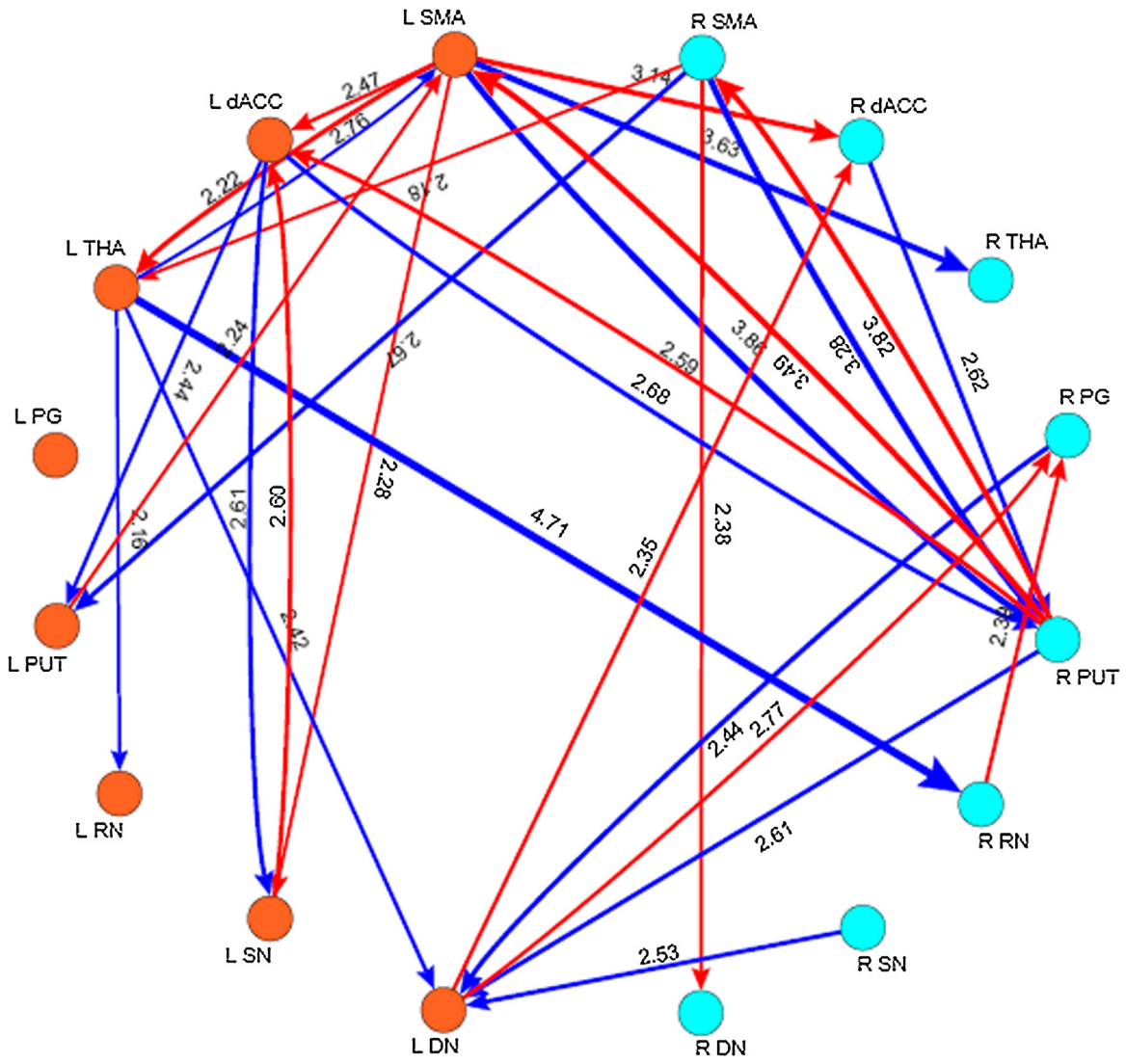


**Fig. 5.** Map of the functional connectivity directions within the extrapyramidal regions inferred by the Granger causality analysis. The red arrows indicate positive influences, and the blue arrows indicate negative influences. The numbers at the middle of each line indicate the *T* value of the path coefficients via a one-sample *t*-test. Thicker arrows indicate higher *T* values. R: right, L: left, SMA: supplementary motor area, dACC: dorsal anterior cingulated cortex, THA: thalamus, PG: globus pallidus, PUT: putamen, SN: substantia nigra, RN: red nucleus, DN: dentate nucleus. (For interpretation of the references to color in this figure legend, the reader is referred to the web version of this article.)

regarding the functional connectivities of the RN, SN and DN remain rare; these gray matter nuclei functionally and anatomically belong to the extrapyramidal system. The functional connectivity maps of the RN, SN and DN primarily embraced the entire extrapyramidal regions. These findings confirmed our hypothesis that the functional connectivity maps are consistent with the extrapyramidal anatomical architectures.

Investigation of extrapyramidal functional networks has potential clinical implications. Changes in the intrinsic extrapyramidal functional networks in PD patients could exert a critical role in PD development and should be investigated in the future.

To date, there are few investigations regarding the functional connectivity maps of the RN, SN and DN possibly because the RN and SN comprise extremely fine and tiny structures in size and the nuclei locations are difficult to position in original fMRI. In our study, this issue was successfully resolved via the combination of fMRI and high resolution SWI. Our method ensured the seeds were appropriately anchored and excluded confusing effects from nearby structures. Our findings suggest that the current method is more accurate compared with previous studies that positioned the seeds on the raw BOLD data.

The primary function of the extrapyramidal system includes the modulation and regulation of movement, muscle tonus and balanced posture. The extrapyramidal system comprises perplexing pathways and feedback loops, with the exclusion of pyramidal pathways. During motor task directed fMRI, the primary motor cortex and extrapyramidal regions may be activated together [24,25], whereas in our results, the resting-state functional connectivity maps of the RN, SN and DN incorporate a series of associated subcortical nuclei, as well as cerebrum cortex regions, such as the SMA, dorsal ACC, supramarginal, insular cortex and cerebellum cortex, other than the primary motor cortex. The distribution of the RN, SN and DN functional maps coincided with the anatomical structures of the extrapyramidal system. Thus, our results demonstrated that the regions involved in the extrapyramidal system constituted a relatively exclusive, functionally tight connection of network system through the cooperation of spatial-temporal signals.

Evidence indicates that the SMA is functionally and anatomically different than the primary motor area; the SMA is important

in motor preparation, whereas the primary motor area is critical in motor execution. Anatomical evidence in macaques indicates that only approximately 10% of corticospinal projections are contributed by the SMA, whereas the primary motor cortex projections are substantially more numerous and exert stronger excitatory effects on corticospinal projections compared with the SMA [26,27]. Thus, these findings indicate the SMA could exhibit a closer relationship to extrapyramidal regions; however, to date, the projection allocation in humans has not been reported. Our findings suggest the SMA is a critical high-order cortical region involved in the extrapyramidal network. PD patients have consistently exhibited reduced SMA activity in neuroimaging studies [19,28–30], and trans-cranial magnetic stimulation of the SMA improved motor functions in PD patients [29,30], as well as motor learning performance in normal subjects [31].

The exploration of Granger causal interactions in neural sources of the time course of network nodes may provide deep insights into brain information processing mechanisms within networks. The dACC comprises cingulated motor areas and projects to the SMA [32]. Our GCA findings indicate the SMA and dACC globally receive positive connectivity from subcortical regions and exert negative influences on subcortical regions with an up-down pattern. Thus, the SMA and dACC are crucial intermediates between motor cortices and subcortical regions. The up-down pattern likely reflects inhibitive and excitative interactions and information feedback within the cortical-basal ganglia-thalamo-cortical loop during the resting state, which maintains a dynamic equilibrium within the extrapyramidal system.

Additionally, our findings indicated that the RN and SN possess close functional connections to the insular cortex and precuneus; these regions are involved in the salience and default mode networks, which are primarily devoted to emotion processing, interoceptive regulation and episodic memory. Thus, when the extrapyramidal networks are impaired, such as in PD, affective and cognitive impairments often coexist.

There are several limitations regarding our methodology. At a TR of 2000 ms, the cardiac and respiratory fluctuation effects might be confounded with the low frequency BOLD MRI signal fluctuations, and this TR may reduce the GCA sensitivity [19]. GCA cannot determine whether the influence between two regions is direct or occurs via other area(s). Thus, our findings do not enable the establishment of an anatomical model of the extrapyramidal loops. Furthermore, the SN, RN and DN are cytoarchitecturally heterogeneous and can be subdivided into subregions; however, the heterogeneity of the nuclei was not assessed.

In summary, our findings suggest that the functional connectivity maps of the RN, SN and DN could primarily reflect the extrapyramidal architectures, which implies functional and anatomical consistencies in the extrapyramidal system.

## Acknowledgements

This work was supported by Grants 30870704, 81471642, 81400899 from the National Natural Science Foundation of China, Grant BE2012706 from Project on Science and Social development of Jiangsu Provincial.

## References

[1] R. de Oliveira-Souza, F. Tovar-Moll, The unbearable lightness of the extrapyramidal system, J. Hist. Neurosci. 21 (2012) 280–292.
[2] R. Oliveira-Souza, Motor hemiplegia and the cerebral organization of movement in man. II. the myth of the human extrapyramidal system, Arq. Neuropsiquiatr. 47 (1989) 16–27.
[3] M.D. Greicius, B. Krasnow, A.L. Reiss, V. Menon, Functional connectivity in the resting brain: a network analysis of the default mode hypothesis, Proc. Natl. Acad. Sci. U. S. A. 100 (2003) 253–258.
[4] M.D. Fox, M. Corbetta, A.Z. Snyder, J.L. Vincent, M.E. Raichle, Spontaneous neuronal activity distinguishes human dorsal and ventral attention systems, Proc. Natl. Acad. Sci. U. S.A. 103 (2006) 10046–10051.
[5] W.W. Seeley, V. Menon, A.F. Schatzberg, J. Keller, G.H. Glover, H. Kenna, et al., Dissociable intrinsic connectivity networks for salience processing and executive control, J. Neurosci. 27 (2007) 2349–2356.
[6] B. Biswal, F.Z. Yetkin, V.M. Haughton, J.S. Hyde, Functional connectivity in the motor cortex of resting human brain using echo-planar MRI, Magn. Reson. Med. 34 (1995) 537–541.
[7] D. Cordes, V.M. Haughton, K. Arfanakis, G.J. Wendt, P.A. Turski, C.H. Moritz, et al., Mapping functionally related regions of brain with functional connectivity MR imaging, AJNR Am. J. Neuroradiol. 21 (2000) 1636–1644.
[8] X.N. Zuo, A. Di Martino, C. Kelly, Z.E. Shehzad, D.G. Gee, D.F. Klein, et al., The oscillating brain: complex and reliable, Neuroimage 49 (2010) 1432–1445.
[9] X. Wang, Y. Jiao, T. Tang, H. Wang, Z. Lu, Investigating univariate temporal patterns for intrinsic connectivity networks based on complexity and low-frequency oscillation: a test-retest reliability study, Neuroscience 254 (2013) 404–426.
[10] J. Cabral, E. Hugues, O. Sporns, G. Deco, Role of local network oscillations in resting-state functional connectivity, Neuroimage 57 (2011) 130–139.
[11] F.D. Bowman, L. Zhang, G. Derado, S. Chen, Determining functional connectivity using fMRI data with diffusion-based anatomical weighting, Neuroimage 62 (2012) 1769–1779.
[12] Z. Wang, Z. Dai, G. Gong, C. Zhou, Y. He, Understanding structural-functional relationships in the human brain: a large-scale network perspective, Neuroscientist (2014).
[13] D. Zhang, A.Z. Snyder, J.S. Shimony, M.D. Fox, M.E. Raichle, Noninvasive functional and structural connectivity mapping of the human thalamocortical system, Cereb. Cortex 20 (2010) 1187–1194.
[14] A. Di Martino, A. Scheres, D.S. Margulies, A.M. Kelly, L.Q. Uddin, Z. Shehzad, et al., Functional connectivity of human striatum: a resting state FMRI study, Cereb. Cortex 18 (2008) 2735–2747.
[15] W.H. Jung, J.H. Jang, J.W. Park, E. Kim, E.H. Goo, O.S. Im, et al., Unravelling the intrinsic functional organization of the human striatum: a parcellation and connectivity study based on resting-state FMRI, PLoS One 9 (2014) e106768.
[16] J. Kong, P.C. Tu, C. Zyloney, T.P. Su, Intrinsic functional connectivity of the periaqueductal gray, a resting fMRI study, Behav. Brain Res. 211 (2010) 215–219.
[17] C. Nioche, E.A. Cabanis, C. Habas, Functional connectivity of the human red nucleus in the brain resting state at 3T, AJNR Am. J. Neuroradiol. 30 (2009) 396–403.
[18] J. Diedrichsen, S. Maderwald, M. Kuper, M. Thurling, K. Rabe, E.R. Gizewski, et al., Imaging the deep cerebellar nuclei: a probabilistic atlas and normalization procedure, Neuroimage 54 (2011) 1786–1794.
[19] T. Wu, J. Wang, C. Wang, M. Hallett, Y. Zang, X. Wu, et al., Basal ganglia circuits changes in parkinson's disease patients, Neurosci. Lett. 524 (2012) 55–59.
[20] K.J. Friston, S. Williams, R. Howard, R.S. Frackowiak, R. Turner, Movement-related effects in fMRI time-series, Magn. Reson. Med. 35 (1996) 346–355.
[21] J.D. Power, K.A. Barnes, A.Z. Snyder, B.L. Schlaggar, S.E. Petersen, Spurious but systematic correlations in functional connectivity MRI networks arise from subject motion, Neuroimage 59 (2012) 2142–2154.
[22] J.P. Hamilton, G. Chen, M.E. Thomason, M.E. Schwartz, I.H. Gotlib, Investigating neural primacy in major depressive disorder: multivariate granger causality analysis of resting-state fMRI time-series data, Mol. Psychiatry 16 (2011) 763–772.
[23] Z.X. Zang, C.G. Yan, Z.Y. Dong, J. Huang, Y.F. Zang, Granger causality analysis implementation on MATLAB: a graphic user interface toolkit for fMRI data processing, J. Neurosci. Methods 203 (2012) 418–426.
[24] P. Wasson, J. Prodoehl, S.A. Coombes, D.M. Corcos, D.E. Vaillancourt, Predicting grip force amplitude involves circuits in the anterior basal ganglia, Neuroimage 49 (2010) 3230–3238.
[25] S. Lehericy, E. Bardinet, L. Tremblay, P.F. Van de Moortele, J.B. Pochon, D. Dormont, et al., Motor control in basal ganglia circuits using fMRI and brain atlas approaches, Cereb. Cortex 16 (2006) 149–161.
[26] R.N. Lemon, M.A. Maier, J. Armand, P.A. Kirkwood, H.W. Yang, Functional differences in corticospinal projections from macaque primary motor cortex and supplementary motor area, Adv. Exp. Med. Biol. 508 (2002) 425–434.
[27] P. Nachev, C. Kennard, M. Husain, Functional role of the supplementary and pre-supplementary motor areas, Nat. Rev. Neurosci. 9 (2008) 856–869.
[28] S.T. Grafton, Contributions of functional imaging to understanding parkinsonian symptoms, Curr. Opin. Neurobiol. 14 (2004) 715–719.
[29] Y. Shirota, H. Ohtsu, M. Hamada, H. Enomoto, Y. Ugawa, Supplementary motor area stimulation for Parkinson disease: a randomized controlled study, Neurology 80 (2013) 1400–1405.
[30] B. Elahi, R. Chen, Effect of transcranial magnetic stimulation on parkinson motor function–systematic review of controlled clinical trials, Mov. Disord. 24 (2009) 357–363.
[31] Y.K. Kim, S.H. Shin, Comparison of effects of transcranial magnetic stimulation on primary motor cortex and supplementary motor area in motor skill learning (randomized, cross over study), Front. Hum. Neurosci. 8 (2014) 937.
[32] J. Tanji, The supplementary motor area in the cerebral cortex, Neurosci. Res. 19 (1994) 251–268.